JCB Journal of Cell Biology

ARTICLE

SGK phosphorylates Cdc25 and Myt1 to trigger cyclin B–Cdk1 activation at the meiotic G2/M transition

Daisaku Hiraoka[1], Enako Hosoda[2], Kazuyoshi Chiba[2], and Takeo Kishimoto[1]

The kinase cyclin B–Cdk1 complex is a master regulator of M-phase in both mitosis and meiosis. At the G2/M transition, cyclin B–Cdk1 activation is initiated by a trigger that reverses the balance of activities between Cdc25 and Wee1/Myt1 and is further accelerated by autoregulatory loops. In somatic cell mitosis, this trigger was recently proposed to be the cyclin A–Cdk1/Plk1 axis. However, in the oocyte meiotic G2/M transition, in which hormonal stimuli induce cyclin B–Cdk1 activation, cyclin A–Cdk1 is nonessential and hence the trigger remains elusive. Here, we show that SGK directly phosphorylates Cdc25 and Myt1 to trigger cyclin B–Cdk1 activation in starfish oocytes. Upon hormonal stimulation of the meiotic G2/M transition, SGK is activated by cooperation between the Gβγ-PI3K pathway and an unidentified pathway downstream of Gβγ, called the atypical Gβγ pathway. These findings identify the trigger in oocyte meiosis and provide insights into the role and activation of SGK.

Introduction

Activation of Cdk1 complexed with cyclin B (cyclin B–Cdk1) induces M-phase entry during mitosis and meiosis (Dunphy and Newport, 1988; Hunt, 1989; Nurse, 1990). Cyclin B–Cdk1 is regulated by synthesis and degradation of cyclin B and by inhibitory phosphorylation of Cdk1 at Thr14 and Tyr15. These residues are phosphorylated by Wee1/Myt1 family kinases but dephosphorylated by Cdc25 (Lew and Kornbluth, 1996). Cyclin B accumulates before and/or during M-phase entry. However, Wee1/Myt1 activity is dominant over Cdc25 activity before M-phase; therefore, cyclin B–Cdk1 remains inactive due to inhibitory phosphorylation. At M-phase entry, a small population of cyclin B–Cdk1 is first activated by a trigger that reverses the balance between Cdc25 and Wee1/Myt1 activities, thereby making Cdc25 activity predominant. Thereafter, cyclin B–Cdk1 itself further accelerates dephosphorylation of Cdk1 via feedback loops, leading to maximal activation (Lew and Kornbluth, 1996; Lindqvist et al., 2009; Qian et al., 2013; Kishimoto, 2015; Hégarat et al., 2016). However, the molecular identity of the trigger of cyclin B–Cdk1 activation remains elusive.

In mitotic M-phase entry (G2/M transition), the trigger may be affected by various factors, such as checkpoints (O'Farrell, 2001; Lindqvist et al., 2009; Rieder, 2011), and may involve redundant or stochastic processes (O'Farrell, 2001; Lindqvist et al., 2009). At least in normal mitotic cell cycles, Plk1 is activated by Aurora A in a cyclin A–Cdk1–dependent manner and, in turn, phosphorylates Cdc25 to trigger activation of cyclin B–Cdk1 (Thomas et al., 2016; Gheghiani et al., 2017; Vigneron et al., 2018). Consistently, the cyclin A–Cdk1/Plk1 axis functions as the trigger in the first embryonic cell division cycle (Okano-Uchida et al., 2003).

Meiotic cell cycles in oocytes mostly arrest at prophase of meiosis I, which corresponds to late mitotic G2 phase (Masui, 1985). Upon extracellular hormonal stimuli, release from this arrest is induced by cyclin B–Cdk1 activation (Kishimoto, 2018); hence, this is known as the meiotic G2/M transition. In contrast with mitotic cell cycles, this transition has not been reported to require cyclin A (Kobayashi et al., 1991; Minshull et al., 1991; Okano-Uchida et al., 1998; Nebreda and Ferby, 2000; Kishimoto, 2003, 2018). Furthermore, Plk1 (Pahlavan et al., 2000; Okano-Uchida et al., 2003; Gaffré et al., 2011) and Aurora (Maton et al., 2003; Abe et al., 2010; Komrskova et al., 2014) are nonessential for transition in some oocytes. Thus, mechanisms other than the cyclin A–Cdk1/Plk1 axis likely trigger cyclin B–Cdk1 activation in oocytes.

In vertebrate oocytes, meiotic G2 arrest requires cAMP-dependent protein kinase A (PKA), and down-regulation of this kinase leads to meiotic G2/M transition (Maller and Krebs, 1977; Nebreda and Ferby, 2000; Jaffe and Egbert, 2017; Kishimoto, 2018). In mice, PKA appears to directly up-regulate Wee1B and down-regulate Cdc25; therefore, activation of cyclin B–Cdk1 might be triggered by a phosphatase that is antagonistic to PKA, rather than by kinases (Adhikari and Liu, 2014). However, the molecular identity and regulation of such a phosphatase are unclear. In *Xenopus laevis*, the hormone

[1]Science and Education Center, Ochanomizu University, Tokyo, Japan; [2]Department of Biological Sciences, Ochanomizu University, Tokyo, Japan.

Correspondence to Daisaku Hiraoka: hiraoka.daisaku@ocha.ac.jp; Takeo Kishimoto: kishimoto.takeo@ocha.ac.jp.

progesterone stimulates protein synthesis of Mos and cyclin B, which redundantly trigger cyclin B–Cdk1 activation (Haccard and Jessus, 2006b): Mos/MAPK cascade activates Cdc25 and newly synthesized cyclin B–associated Cdk1 inactivates Myt1 (Gaffré et al., 2011). However, the molecular link between down-regulation of PKA and de novo synthesis of Mos and cyclin B remains elusive (Haccard and Jessus, 2006a; Dupré et al., 2014).

In contrast with vertebrate oocytes, the mechanisms of the trigger at the meiotic G2/M transition have been well studied in invertebrate starfish oocytes since the existence of a trigger kinase was first reported (Okumura et al., 1996; Kishimoto, 2003, 2018). In starfish, cAMP and PKA are unlikely to be involved in meiotic G2 arrest (Meijer and Guerrier, 1984). The physiological maturation-inducing hormone 1-methyladenine (1-MeAde) induces the meiotic G2/M transition (Kanatani et al., 1969) without a requirement for new protein synthesis (Dorée, 1982). Cyclin A, Wee1, and Mos are not present, and Aurora and Plk are not required for cyclin B–Cdk1 activation in the meiotic G2/M transition (Okano-Uchida et al., 1998, 2003; Tachibana et al., 2000; Abe et al., 2010). In unstimulated oocytes, cyclin B is already accumulated (Ookata et al., 1992), but Myt1 inactivates cyclin B–Cdk1 (Okumura et al., 2002). 1-MeAde stimulates an unidentified cell surface G protein–coupled receptor (GPCR) to dissociate Gβγ from Gαi on the plasma membrane (Kanatani and Hiramoto, 1970; Shilling et al., 1989; Chiba et al., 1993; Jaffe et al., 1993). Gβγ binds to and activates phosphoinositide-3-kinase (PI3K), resulting in production of phosphatidylinositol 3,4,5-triphosphate (PI-345P_3; Sadler and Ruderman, 1998; Vanhaesebroeck et al., 2010). Dependent on PI-345P_3, phosphoinositide-dependent kinase 1 (PDK1) and target of rapamycin complex 2 (TORC2) phosphorylate Akt in its activation loop (A-loop) and hydrophobic motif (HM), respectively, leading to its activation (Hiraoka et al., 2004, 2011). Thereafter, Akt inactivates Myt1 by directly phosphorylating Ser75 (Okumura et al., 2002) and activates Cdc25 by directly phosphorylating multiple residues including Ser188 (Hiraoka et al., 2016), resulting in reversal of the balance of Cdc25 and Myt1 activities, and consequently initial activation of cyclin B–Cdk1 (Okumura et al., 1996, 2002). These observations suggest that Akt likely represents the trigger kinase at the meiotic G2/M transition in starfish oocytes (Okumura et al., 2002).

Nevertheless, our recent observations suggest that the PI3K-Akt pathway is insufficient (Hiraoka et al., 2016). Expression of a constitutively active form of Akt induces the meiotic G2/M transition, but its required expression level is 40-fold higher than that of endogenous Akt. Furthermore, expression of a constitutively active form of PI3K (CA-PI3K) induces Akt activation but results in low levels of Cdc25 and Myt1 phosphorylation, and therefore fails to induce the meiotic G2/M transition. We reported that another pathway, called "the atypical pathway," which is activated by Gβγ in parallel with PI3K activation, compensates for this insufficiency (Hiraoka et al., 2016). Although the molecular details of this pathway remain unclear, we proposed that it cooperates with the PI3K-Akt pathway to trigger cyclin B–Cdk1 activation (Hiraoka et al., 2016). One possibility is that another kinase, which can redundantly phosphorylate Akt substrates, functions in these pathways to trigger cyclin B–Cdk1 activation.

Candidates for such a kinase are p90 ribosomal S6 kinase, p70 ribosomal S6 kinase (p70S6K), and serum- and glucocorticoid-regulated kinase (SGK). Along with Akt, they belong to the AGC kinase family and share a redundant substrate consensus sequence (Pearce et al., 2010). However, p70S6K is unlikely to be required for cyclin B–Cdk1 activation because inhibition of TORC1, a well-known upstream kinase of p70S6K, by rapamycin does not affect the meiotic G2/M transition in oocytes (Hiraoka et al., 2011). p90 ribosomal S6 kinase is also unlikely to be the trigger kinase in starfish oocytes because it is activated after cyclin B–Cdk1 (Okumura et al., 2002). By contrast, SGK could be a possible candidate. In mammalian cells, similar to Akt, SGK family members are activated in a PI3K-dependent manner, dependent on phosphorylation of the A-loop and HM by PDK1 and TORC2, respectively (Webster et al., 1993; Kobayashi and Cohen, 1999; García-Martínez and Alessi, 2008; Pearce et al., 2010; Lien et al., 2017). However, the contribution of SGK to the meiotic G2/M transition has not been investigated.

Here, we carefully evaluated whether Akt and SGK play redundant roles in the meiotic G2/M transition in starfish oocytes. We showed that SGK is necessary and sufficient for the initial phosphorylation of Cdc25 and Myt1 to trigger cyclin B–Cdk1 activation upon 1-MeAde stimulation. By contrast, although contradictory to our previous report (Okumura et al., 2002), Akt was dispensable for the meiotic G2/M transition. Several experiments supported the importance of SGK, rather than Akt. This discrepancy is discussed here. Furthermore, as upstream pathways, we found that PI3K and the atypical Gβγ pathway cooperatively activate SGK. All these observations clearly explain the insufficiency of the PI3K-Akt pathway. Thus, our findings indicate that SGK is the trigger kinase at the meiotic G2/M transition in starfish oocytes and provide new insights into SGK activation.

Results

A newly generated phospho-specific antibody detects A-loop phosphorylation of starfish Akt (sfAkt) and of starfish SGK (sfSGK)

In previous studies (Hiraoka et al., 2011, 2016), we monitored phosphorylation of the HM by immunoblotting as a marker of Akt activity in starfish oocytes because of lack of an antibody that detects the phosphorylated A-loop. Nevertheless, it is important to analyze A-loop phosphorylation to precisely evaluate Akt activation. Thus, we attempted to generate a phospho-specific antibody against a 17-aa phospho-peptide derived from the A-loop of sfAkt that includes phospho-Thr at the site of phosphorylation by PDK1 (Figs. 1 A and S1 A). In immunoblot analysis of whole-oocyte samples using this antibody, phosphorylation of Akt was detectable following 1-MeAde stimulation only when Akt was overexpressed (Fig. 1 B, closed arrowhead). When endogenous Akt was concentrated by immunoprecipitation using an antibody raised against a C-terminal fragment of sfAkt (anti-sfAkt-C antibody), the anti-phospho-A-loop antibody detected a band at

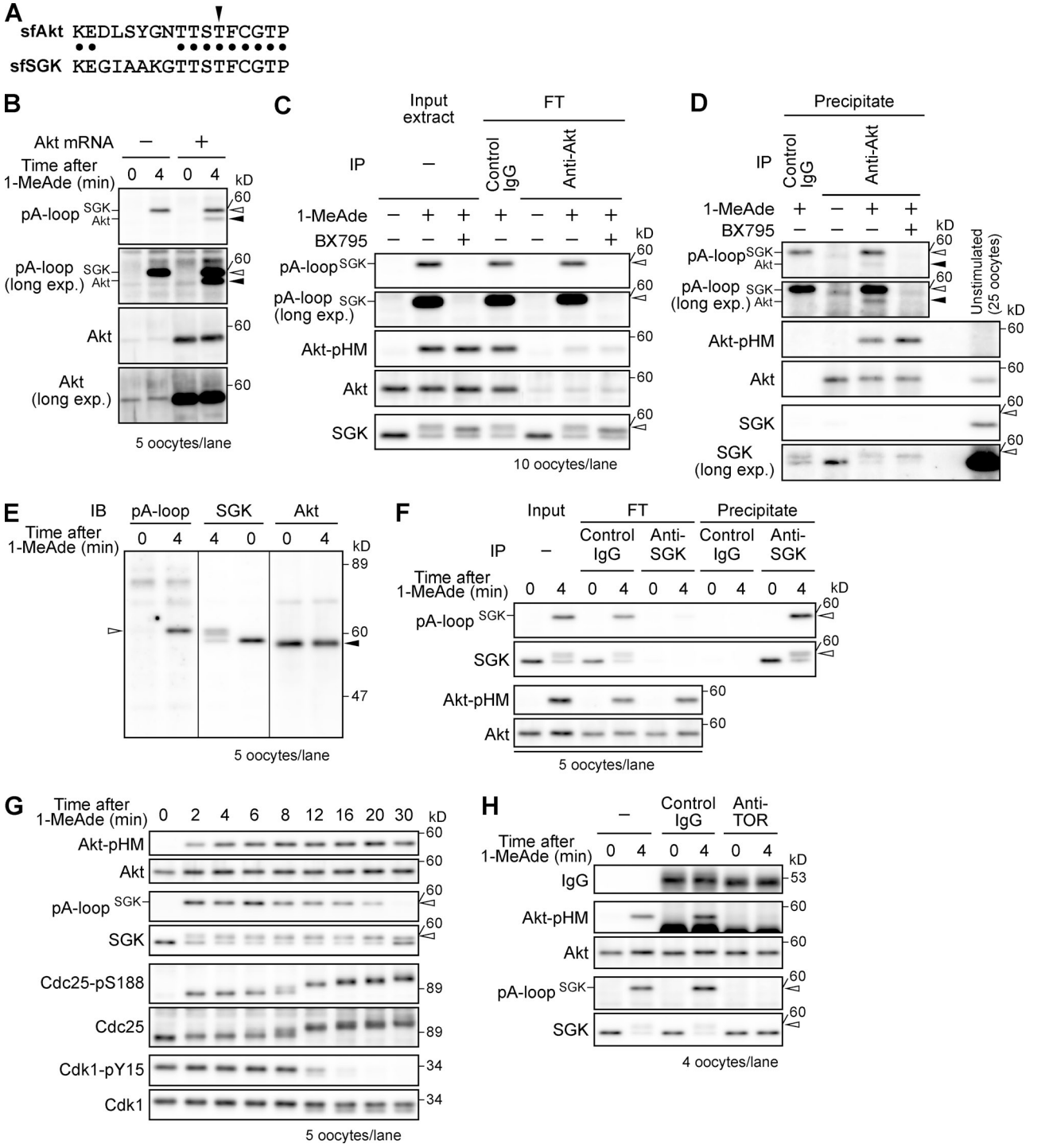

Figure 1. **SGK is activated after 1-MeAde stimulation in a PDK1- and TORC2-dependent manner. (A)** The region of sfAkt used to raise the anti-phospho-A-loop antibody (Lys304–Pro320 of sfAkt) is aligned with the corresponding region of sfSGK (Lys301–Pro317; see also Fig. S1 A). The arrowhead indicates the residue phosphorylated by PDK1. Dots indicate identical residues. **(B)** A-loop phosphorylation of endogenous sfAkt is undetectable in whole oocyte extracts. Oocytes injected with or without sfAkt-mRNA were treated with 1-MeAde and analyzed by immunoblotting with the anti-phospho-A-loop (pA-loop) and anti-sfAkt-C (Akt) antibodies. Closed arrowheads indicate A-loop phosphorylation of Akt. Open arrowheads indicate the positions of active SGK (see E and F). exp., exposure. **(C and D)** A-loop phosphorylation of endogenous Akt is detectable in immunoprecipitates. Oocytes were incubated with 1-MeAde in the presence or absence of a PDK1 inhibitor, BX795, and subjected to immunoprecipitation with control IgG or the anti-sfAkt-C antibody. Input and flow-through (FT) extracts (C) and precipitates (D) were analyzed by immunoblotting (Akt-pHM represents phosphorylation of Ser477 in the HM of Akt). Closed arrowheads in D indicate A-loop phosphorylation of Akt. A-loop phosphorylation of nonspecifically included SGK was detected in both control and Akt immunoprecipitates (D, open arrowheads in pA-loop). IP, immunoprecipitation. **(E)** Unstimulated and 1-MeAde–treated oocytes were subjected to immunoblotting (IB) with anti-phospho-A-loop (left), anti-sfSGK-HM (middle), and anti-sfAkt-C (right) antibodies. Closed and open arrowheads indicate positions of Akt and active SGK, respectively. **(F)** The anti-phospho-A-loop antibody against sfAkt cross-reacts with A-loop-phosphorylated endogenous SGK. Oocytes were treated with 1-MeAde.

Immunoprecipitation was performed with control IgG or the anti-sfSGK-HM antibody. **(G)** SGK is activated simultaneously with Akt activation. Oocytes were treated with 1-MeAde for indicated durations and analyzed by immunoblotting. GVBD occurred at ∼20 min. **(H)** SGK activation depends on TOR. Oocytes were injected with control IgG or the anti-TOR antibody, treated with 1-MeAde, and analyzed by immunoblotting. Open arrowheads in B–H indicate the position of active SGK. The data are representative of two independent experiments in B, E, F, and H and three independent experiments in C, D, and G. Full blots for B–H are presented in Fig. S5.

the same size as Akt after 1-MeAde stimulation (Fig. 1, C and D, for input and flow-through and for precipitate [closed arrowhead], respectively). The band disappeared upon treatment with the PDK1 inhibitor BX795 (Fig. 1 D, closed arrowhead), indicating that the anti-phospho-A-loop antibody successfully detected A-loop phosphorylation of endogenous Akt by PDK1.

The phospho-A-loop antibody detected another band that migrated slightly slower (∼60 kD) than Akt (Fig. 1, B and C, open arrowhead). This band was still observed in flow-through samples in which Akt had been removed by immunoprecipitation (Fig. 1 C, open arrowhead), indicating that the band does not correspond to Akt.

In parallel with our study, Hosoda et al. found that SGK is activated after 1-MeAde stimulation in starfish oocytes in a study of intracellular pH regulation. They isolated a cDNA encoding sfSGK (predicted molecular weight, 56 kD) and collaborated with us to generate an anti-sfSGK neutralizing antibody raised against a C-terminal peptide of sfSGK including the HM (anti-sfSGK-HM antibody; Fig. S1 A). Based on the following observations using this antibody, we concluded that the additional band detected by the anti-phospho-A-loop antibody corresponds to A-loop phosphorylation of SGK: (a) the mobility of this band was the same as that of the top band of SGK detected by the anti-sfSGK-HM antibody in 1-MeAde–treated oocytes (Fig. 1 E, open arrowhead); (b) the band disappeared after immunodepletion of SGK from oocyte extracts, whereas it appeared in immunoprecipitates of SGK (Fig. 1 F); (c) 11 of the 17 residues in the antigen of the anti-phospho-A-loop antibody are conserved in sfSGK (Figs. 1 A and S1 A); and (d) the anti-phospho-A-loop antibody recognized the phospho-A-loop peptide derived from not only sfAkt but also sfSGK in dot blot analysis of dilution series of the synthetic peptides, although its sensitivity to sfSGK was threefold lower than to sfAkt (Fig. S1 B).

SGK and Akt phosphorylate a Ser or Thr residue in the same consensus motif (RXRXXS/T, where X represents any amino acid; Kobayashi and Cohen, 1999) and may therefore play a redundant role in 1-MeAde signaling. Thus, we further analyzed the role and regulation of SGK.

SGK is activated after 1-MeAde stimulation simultaneously with Akt in a PDK1- and TORC2-dependent manner

We first analyzed the time of SGK activation in detail. As we showed previously (Hiraoka et al., 2016), phosphorylation of Akt in the HM and phosphorylation of Cdc25 at Ser188 were detected within 2 min after 1-MeAde addition (Fig. 1 G). Thereafter, Tyr15 of Cdk1 was dephosphorylated, indicating cyclin B–Cdk1 activation (Fig. 1 G, 12 min and later). SGK was activated at a similar time to Akt, ahead of cyclin B–Cdk1 activation (Fig. 1 G, pA-loop).

We then examined activators of SGK. In mammalian cells, SGK is activated by phosphorylation of its A-loop and HM by PDK1 and mTORC2, respectively (Kobayashi and Cohen, 1999; García-Martínez and Alessi, 2008). In addition, A-loop phosphorylation depends on HM phosphorylation (Kobayashi and Cohen, 1999). In starfish oocytes, BX795 inhibited A-loop phosphorylation of SGK, indicating that this phosphorylation depends on PDK1 (Fig. 1 C). A mobility shift of SGK was still observed even in the absence of A-loop phosphorylation upon BX795 treatment (Fig. 1 C). Using chemical inhibitors, Hosoda et al. (2019) suggested that this shift represents TORC2-dependent phosphorylation. Consistently, inhibition of TOR by an anti-TOR neutralizing antibody (Hiraoka et al., 2011) completely abolished both A-loop phosphorylation and the mobility shift (Fig. 1 H). Therefore, A-loop phosphorylation of SGK likely depends on TORC2-dependent HM phosphorylation in starfish oocytes, as reported in mammals.

SGK, but not Akt, is required for the meiotic G2/M transition

Next, we examined the involvement of Akt and SGK in the meiotic G2/M transition using antibodies that inhibit each kinase specifically. The anti-sfAkt-C antibody detected nonspecific bands by immunoblotting, but did not in its immunoprecipitates (Fig. 2 A), indicating that this antibody does not interact with these nonspecific proteins in nondenaturing conditions. In addition, although immunoprecipitates obtained using the anti-sfAkt-C antibody contained a trace amount of SGK (Fig. 1 D, SGK with long exposure), this was not due to cross-reaction of SGK with this antibody because a similar amount of SGK was detected in a control precipitation obtained using a control IgG (Fig. 1 D, SGK with long exposure). These observations confirm the specificity of the anti-sfAkt-C antibody. The anti-sfSGK-HM antibody specifically detected SGK by immunoblotting (Fig. 1 E). In addition, the protein level of Akt remained constant before and after depletion of SGK using this antibody (Fig. 1 F), confirming the specificity of the anti-sfSGK-HM antibody.

The antigens of these antibodies include the phosphorylation site in the HM of each protein (Fig. S1 A). Thus, we expected the antibodies to bind to the HM and block its phosphorylation. Indeed, injection of the anti-sfAkt-C antibody abolished HM phosphorylation of Akt (Fig. 2 B). Consistent with our previous suggestion that A-loop phosphorylation of Akt depends on its HM phosphorylation in starfish oocytes (Hiraoka et al., 2011), A-loop phosphorylation was also disrupted by injection of the anti-sfAkt-C antibody (Fig. 2 C). SGK was activated as normal in these oocytes (Fig. 2 B). Thus, the anti-sfAkt-C antibody specifically inhibits Akt activation. On the other hand, the anti-sfSGK-HM antibody disrupted both A-loop phosphorylation and the mobility shift of SGK (Fig. 2 D) without affecting phosphorylation of Akt (Fig. 2, panel D for HM and E for A-loop), indicating that this antibody specifically inhibits SGK activation.

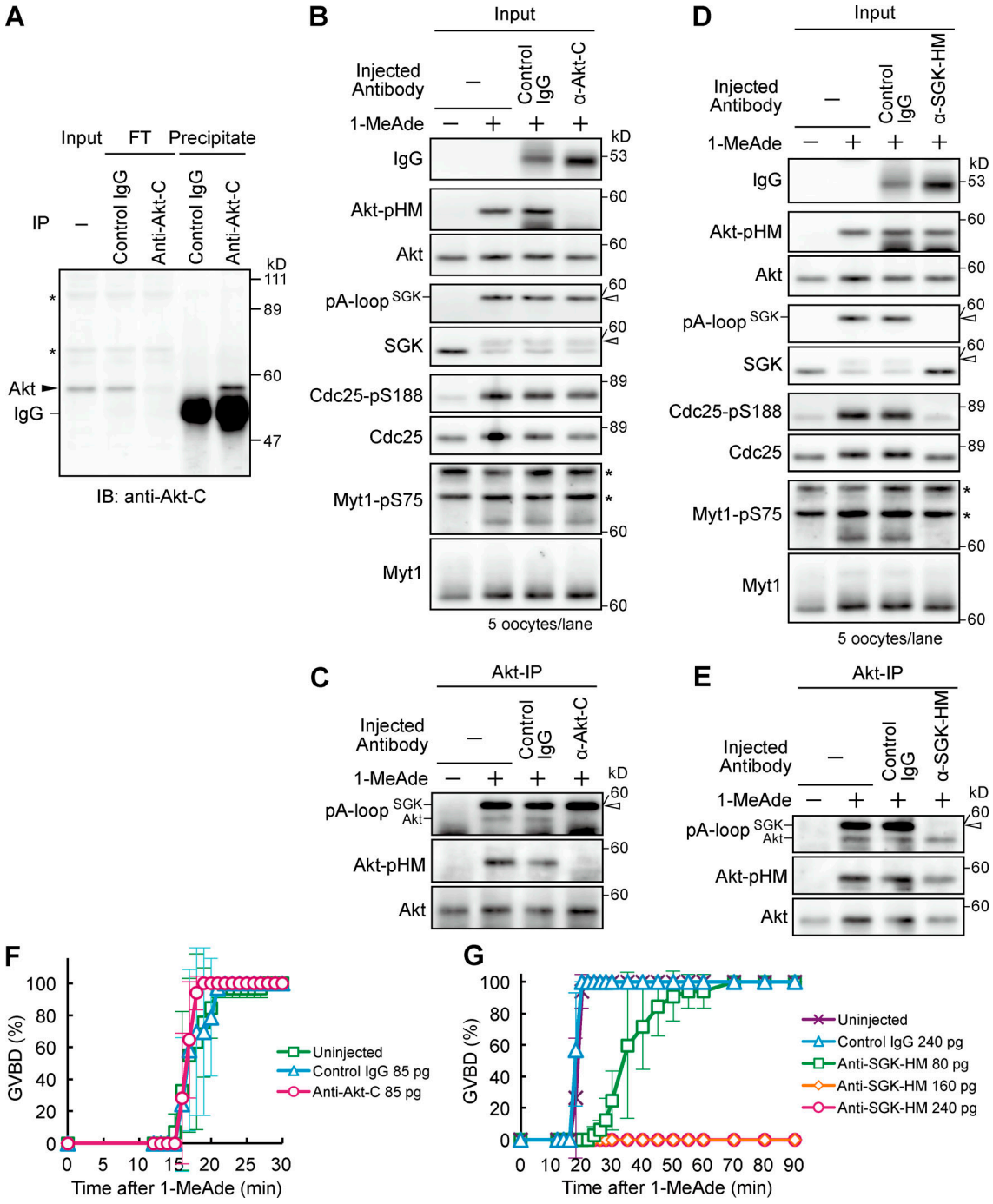

Figure 2. **SGK, but not Akt, is required for the meiotic G2/M transition. (A)** Immunoprecipitation (IP) with control IgG or the anti-sfAkt-C antibody was performed using extracts of unstimulated oocytes, followed by immunoblotting (IB) with the anti-sfAkt-C antibody. FT, flow-through. **(B–E)** Inhibition of activation of Akt and SGK by specific antibodies. Oocytes were injected with the anti-sfAkt-C antibody (B and C), the anti-sfSGK-HM antibody (D and E), or control IgG (B–E) and then treated with 1-MeAde for 4 min. Immunoprecipitation with the anti-sfAkt-C antibody was performed. Input extracts (B and D) and precipitates (C and E) were analyzed by immunoblotting. Open arrowheads indicate the position of active SGK. Asterisks indicate nonspecific bands. The data are representative of two independent experiments in A–C and three independent experiments in D and E. **(F and G)** SGK, but not Akt, is required for the meiotic G2/M transition. Oocytes were injected with the anti-sfAkt-C antibody (F), the anti-sfSGK-HM antibody (G), or control IgG (F and G) and then treated with 1-MeAde. GVBD was monitored as a marker of the meiotic G2/M transition. The graphs show the percentage of oocytes that had undergone GVBD by the indicated time points (mean ± SD from three independent experiments). Full blots for A–E are presented in Fig. S6.

We next examined the effect of inhibition of SGK or Akt by each antibody on the meiotic G2/M transition. As a marker of the meiotic G2/M transition, we monitored germinal vesicle breakdown (GVBD), which is equivalent to nuclear envelope breakdown in somatic cells. Surprisingly, GVBD occurred as normal in the Akt-inhibited oocytes (Fig. 2 F). By contrast, GVBD

was suppressed in the SGK-inhibited oocytes (Fig. 2 G), suggesting that SGK, but not Akt, is required for the meiotic G2/M transition.

We previously reported that injection of an anti-sfAkt antibody inhibits the meiotic G2/M transition (Okumura et al., 2002). The antibody in that previous study was raised against an 88-aa C-terminal fragment of sfAkt. In the present study, there were no stocks of the antiserum left and therefore we used an antibody raised against the same antigen in another rabbit. Thus, the specificity of the previous antibody may differ from that of the present one. Since 33 of the 88 residues in the antigen are conserved in sfSGK (Fig. S1 A), the previous antibody may have cross-reacted with SGK and consequently inhibited SGK as well as Akt. Checking the previous antibody's specificity was limited during our previous study because we lacked the antibodies to detect SGK and phosphorylation of these kinases. To confirm our conclusion, we raised new antibodies by immunizing two rabbits against the C-terminal 16-aa peptide of sfAkt including the HM (anti-sfAkt-HM antibody; Figs. S1 A and S2 A). Injection of these antibodies inhibited Akt activation (Fig. S2 B) but did not affect GVBD (Fig. S2 C). These findings further support our conclusion that Akt is not essential for the meiotic G2/M transition.

SGK directly phosphorylates Cdc25 and Myt1 to trigger cyclin B–Cdk1 activation

To trigger activation of cyclin B–Cdk1, we previously demonstrated that Cdc25 and Myt1 are activated and inactivated, respectively, by phosphorylation of Akt/SGK consensus motifs: multiple sites including Ser188 in Cdc25 (Hiraoka et al., 2016) and Ser75 in Myt1 (Okumura et al., 2002). Consistent with the requirement of SGK for the meiotic G2/M transition, phosphorylation of Cdc25 at Ser188 and Myt1 at Ser75 was abolished by inhibition of SGK (Fig. 2 D) but not by inhibition of Akt (Figs. 2 B and S2 B). Furthermore, in Phos-tag SDS-PAGE, which emphasizes the mobility shifts of phosphorylated proteins, the upward shifts of Cdc25 and Myt1 after 1-MeAde stimulation were completely suppressed by inhibition of SGK but not of Akt (Fig. 3 A). This suggests that the regulatory phosphorylation of Cdc25 and Myt1 to trigger activation of cyclin B–Cdk1 depends on SGK but not on Akt.

To investigate whether SGK directly phosphorylates Cdc25 and Myt1, in vitro phosphorylation experiments were performed using recombinant proteins. Attempts to prepare active recombinant sfSGK were unsuccessful; therefore, we used commercially available recombinant human SGK3 (hSGK3), which is the best related to sfSGK among the three isoforms of hSGK (Hosoda et al., 2019). Ser188 of starfish Cdc25 was phosphorylated upon incubation with hSGK3 (Fig. 3 B). In addition, the mobility shift was still observed on the S188A mutant (Fig. 3 B), suggesting that hSGK3 directly phosphorylates Cdc25 at multiple residues including Ser188. hSGK3 also phosphorylated Ser75 of starfish Myt1, leading to a slight mobility shift (Fig. 3 C). The shift of Myt1 was not observed on the S75A mutant (Fig. 3 C), suggesting that Ser75 is the only site phosphorylated by hSGK3 in Myt1. Furthermore, peptide substrates derived from starfish Cdc25 including Ser188 and from starfish Myt1

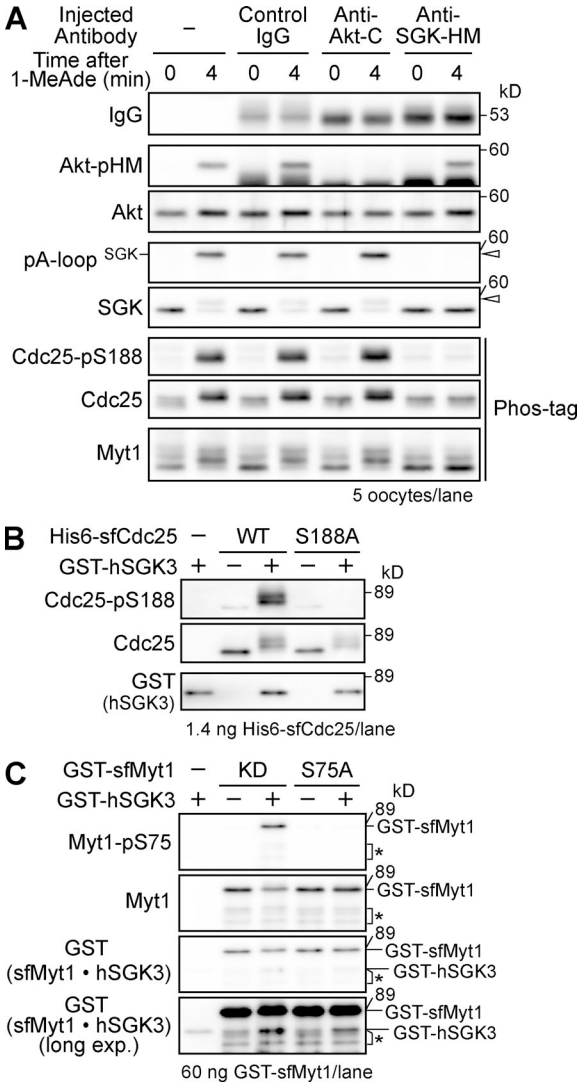

Figure 3. **SGK directly phosphorylates Cdc25 and Myt1. (A)** SGK, but not Akt, is required for Cdk-independent phosphorylation of Cdc25 and Myt1 upon 1-MeAde stimulation. Oocytes were injected with the indicated antibodies, treated with 1-MeAde in the presence of roscovitine, and then analyzed by immunoblotting using a normal or Phos-tag–containing SDS-PAGE gel. Open arrowheads indicate position of active SGK. **(B)** His-tagged recombinant WT sfCdc25 or the S188A mutant was incubated with or without GST-tagged active hSGK3 in the presence of ATP and $MgCl_2$. Thereafter, immunoblotting was performed. **(C)** GST-tagged recombinant kinase-dead (KD) or the S75A mutant of sfMyt1 was phosphorylated by hSGK3 as described in B. Asterisks indicate minor fragments of recombinant Myt1. The data in A–C are representative of two independent experiments. Full blots for A–C are presented in Fig. S7.

including Ser75 were phosphorylated upon incubation in extracts prepared from 1-MeAde–treated oocytes, but not upon incubation in an extract from which SGK had been removed by immunodepletion (Fig. S3), indicating that endogenous sfSGK phosphorylated these peptides in the extract. Taken together, these results suggest that Cdc25 and Myt1 are substrates for SGK in starfish oocytes.

Contribution of Akt to meiotic G2/M transition was undetectable in the present study even though it can phosphorylate

Cdc25 and Myt1 in vitro (Okumura et al., 2002; Hiraoka et al., 2016) and was activated after 1-MeAde stimulation (Okumura et al., 2002; see also Fig. 1). A simple explanation would be that Akt activity is very weak. This was supported by experiments using oocyte extracts. A GST-conjugated, commonly used Akt/SGK substrate peptide was phosphorylated in the extract of 1-MeAde–treated oocytes (Fig. 4, A and B). This phosphorylation of the peptide was not affected by immunodepletion of Akt (Fig. 4, C–E), but was abolished upon depletion of SGK (Fig. 4, F–H). Therefore, SGK, but not Akt, is responsible for the detected kinase activity. Akt activity in oocyte extracts was only detectable when Akt was overexpressed by injection of mRNA in SGK-inhibited oocytes (Fig. S4). We compared A-loop phosphorylation levels and activities between endogenous SGK and overexpressed Akt. Based on this comparison, we roughly estimated that the concentration and total activity of active endogenous SGK were >200-fold higher than those of active endogenous Akt (for details, see the Fig. S4 legend).

Together, these observations support the conclusion that SGK, but not Akt, is required for the regulatory phosphorylation that makes Cdc25 activity dominant over Myt1 activity to trigger cyclin B–Cdk1 activation.

SGK is sufficient for the regulatory phosphorylation of Cdc25 and Myt1 to trigger cyclin B–Cdk1 activation at the meiotic G2/M transition

Next, we investigated whether SGK is sufficient to trigger cyclin B–Cdk1 activation. Mammalian SGK3 and sfSGK have a phox homology domain (PX domain; Fig. S1 A; Liu et al., 2000; Hosoda et al., 2019). Upon agonist stimuli, binding of PX domain to phosphoinositides on the cellular membrane contributes to activation of mammalian SGK3 (Virbasius et al., 2001; Lien et al., 2017). To generate the constitutively active form of sfSGK (CA-SGK), we substituted the PX domain of sfSGK with a myristoylation sequence for membrane-targeting. Furthermore, Thr479, the phosphorylation site by TORC2, was substituted with Glu to mimic phosphorylation of the HM. Expression of the CA-SGK in unstimulated oocytes induced GVBD (Fig. 5 A). The level of A-loop phosphorylation of CA-SGK at GVBD in these oocytes was comparable to that of endogenous SGK in 1-MeAde–treated intact oocytes (Fig. 5, B and C), suggesting that endogenous levels of SGK activation is sufficient for the meiotic G2/M transition.

We then examined whether CA-SGK induces the regulatory phosphorylation of Cdc25 and Myt1 to trigger cyclin B–Cdk1 activation. CA-SGK was expressed in the presence of the Cdk inhibitor roscovitine to avoid any effect of Cdk-dependent feedback pathways. Phosphorylation of Cdc25 at Ser188 and of Myt1 at Ser75 were detectable in the oocytes even when expression and A-loop phosphorylation levels of CA-SGK were still lower than those of endogenous SGK (Fig. 5 D). These results suggest that activation of SGK is sufficient for the regulatory phosphorylation of Cdc25 and Myt1 to trigger cyclin B–Cdk1 activation.

The Gβγ-PI3K and atypical Gβγ pathways cooperatively activate SGK in starfish oocytes

Previously, we proposed the existence of an atypical Gβγ pathway that is activated by Gβγ and cooperates with the Gβγ-PI3K pathway to induce the meiotic G2/M transition (Hiraoka et al., 2016). We then examined whether SGK is activated by these pathways.

First, we investigated whether signaling from Gβγ can activate SGK. Expression of exogenous Gβγ induced the meiotic G2/M transition as previously reported (Fig. 6 A; Hiraoka et al., 2016). Similarly to 1-MeAde stimulation, this induction was dependent on SGK, but not Akt, as indicated by injection of the neutralizing antibodies (Fig. 6 A). Consistently, SGK was activated upon expression of Gβγ (Fig. 6 B, pA-loop). This activation was independent of Cdk activity because it occurred even in the presence of the Cdk inhibitor roscovitine (Fig. 6 C). However, 1-MeAde– and Gβγ-induced SGK activation was abolished upon inhibition of PI3K by wortmannin (Fig. 6 D), suggesting that activation of SGK by Gβγ requires PI3K.

Next, to determine whether PI3K activation solely induces SGK activation, CA-PI3K was expressed in unstimulated oocytes. As previously reported (Hiraoka et al., 2016), CA-PI3K induced HM phosphorylation of Akt (Fig. 6 E), but not the meiotic G2/M transition. In these oocytes, A-loop phosphorylation of SGK was only detectable by immunoblotting with a long time exposure (Fig. 6 E, pA-loop with long exposure, open arrowhead), indicating that activation of PI3K barely induces activation of SGK.

Taken together, Gβγ activates SGK in a PI3K-dependent manner, but activation of PI3K alone is insufficient for SGK activation. These observations suggest that Gβγ activates not only PI3K but also another pathway (or multiple pathways), which we call the atypical Gβγ pathway, and that cooperation of the Gβγ-PI3K and atypical Gβγ pathways activates SGK.

As to activation of Akt, we found that a weak A-loop phosphorylation of Akt was detectable (confirmed by immunodepletion of Akt) upon CA-PI3K expression in immunoblot with a long exposure (Fig. 6 E, closed arrowhead) even in whole-oocyte samples. Given that the 1-MeAde–induced A-loop phosphorylation of Akt was below the threshold of detection in whole-oocyte samples (Fig. 1, B–D), Akt is activated more strongly by CA-PI3K than by 1-MeAde. This further supports that activation of endogenous Akt is insufficient for the meiotic G2/M transition. By contrast, A-loop phosphorylation of Akt by Gβγ expression was undetectable even in immunoprecipitated Akt samples (Fig. 6 F), although HM phosphorylation was comparable to that by 1-MeAde stimulation (Fig. 6 C, Akt-pHM). This suggests that Gβγ signaling is insufficient for A-loop phosphorylation of Akt. This finding will be discussed later.

Discussion

This study showed that SGK is necessary and sufficient for the regulatory phosphorylation of Cdc25 and Myt1 to trigger activation of cyclin B–Cdk1 in the meiotic G2/M transition. Furthermore, we revealed that SGK is activated by cooperation of the Gβγ-PI3K and atypical Gβγ pathways downstream of 1-MeAde stimulation (Fig. 7). These findings clarify the molecular identity of the trigger kinase and offer important clues to elucidate the 1-MeAde signaling pathway. Moreover, they provide new insights into the role and regulation of SGK.

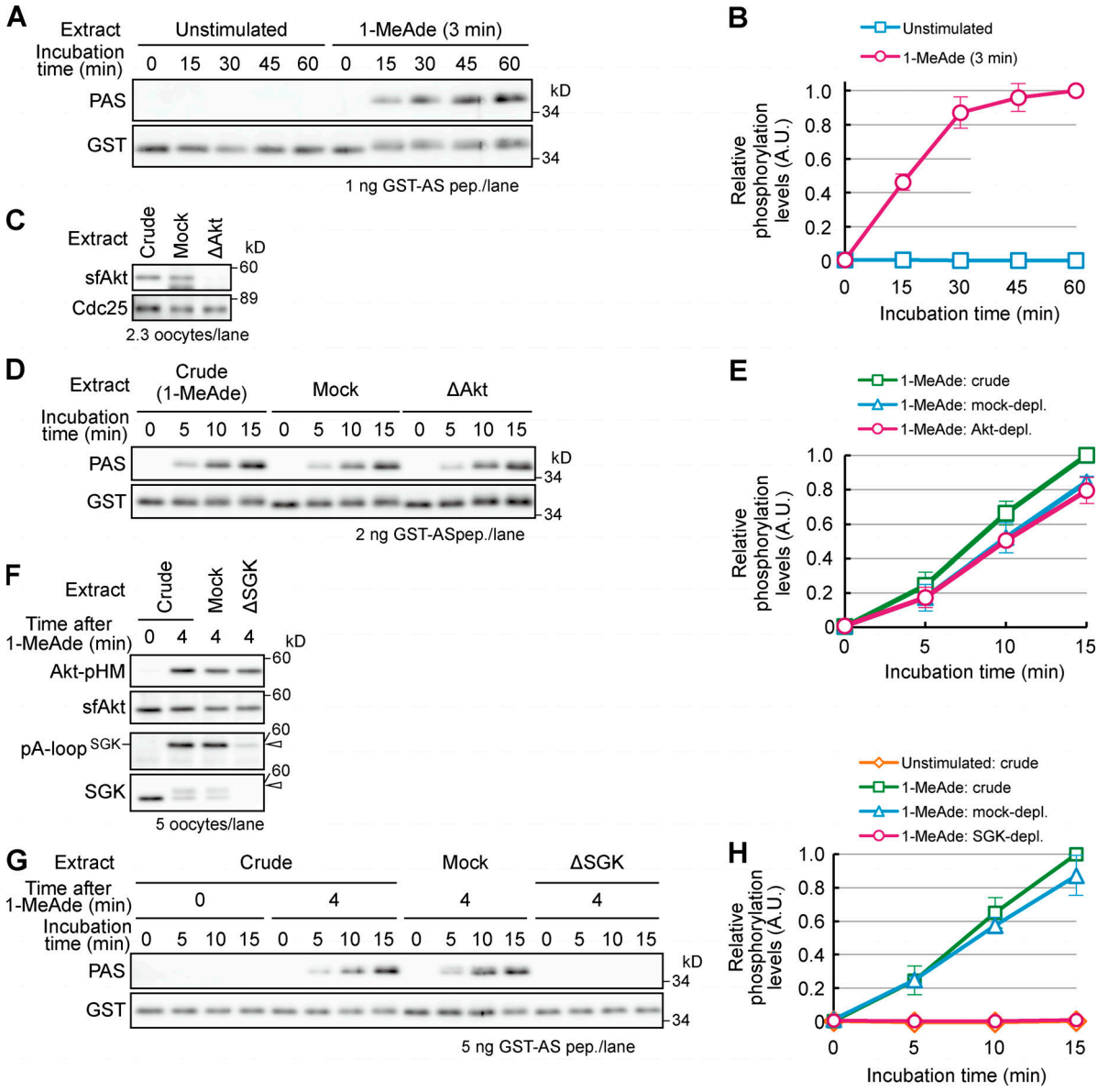

Figure 4. **SGK is the major kinase that phosphorylates the Akt/SGK consensus motif in starfish oocytes. (A and B)** Kinase activity for the AS peptide is detectable in an extract of 1-MeAde–treated oocytes. Extracts were prepared from unstimulated or 1-MeAde–treated (3 min) oocytes and incubated with the GST-AS peptide for the indicated durations. Phosphorylation of the peptide was detected by immunoblotting with an anti-pan-phospho-Akt/SGK substrate antibody (PAS), which recognizes phosphorylated Ser or Thr in the Akt/SGK consensus motif (A). Phosphorylation of the peptide was quantitated from the blots in A and normalized against the total amount of the peptide. The graph shows the levels of phosphorylation relative to that at 60 min (B; mean ± SD from three independent experiments). **(C–H)** SGK, but not Akt, is responsible for the detectable AS-peptide kinase activity in the extract. An extract was prepared from 1-MeAde–treated oocytes (Crude). Immunodepletion was performed with control IgG (mock), the anti-sfAkt-C antibody (ΔAkt), or the anti-sfSGK-HM antibody (ΔSGK). Immunoblot of the extracts (C and F) and GST-AS peptide kinase assay using the extracts (D and G) are shown. Phosphorylation was quantitated as described in A and B. Graphs show the levels of phosphorylation relative to those at 15 min in the crude extract of 1-MeAde–treated oocytes (E from the blot in D, and H from the blot in G; mean ± SD from three independent experiments). Open arrowheads in F indicate the position of active SGK. Full blots for A, C, D, F, and G are presented in Fig. S7.

In *Xenopus* oocytes, multiple pathways are proposed to reverse the balance between the activities of Cdc25 and Myt1 (Haccard and Jessus, 2006b; Gaffré et al., 2011). Therefore, it is difficult to determine the relative contribution of each pathway. In this context, SGK is most likely the main trigger kinase in starfish oocytes because (a) it was necessary and sufficient for the regulatory phosphorylation of Cdc25 and Myt1 (Figs. 2, 3, and 5); (b) phosphorylation of Cdc25 and Myt1 was undetectable in SGK-inhibited oocytes (Fig. 2 D); and (c) it was responsible for the kinase activities in oocyte extracts that phosphorylated a commonly used Akt/SGK substrate and sfMyt1-derived and sfCdc25-derived peptides (Figs. 4 and S3). In mouse oocytes, the identity of a putative phosphatase, which antagonizes PKA and functions as the trigger, remains to be elucidated (Adhikari and Liu, 2014). Thus, the present study is the first to clarify the trigger kinase in oocyte meiosis. Furthermore, to our

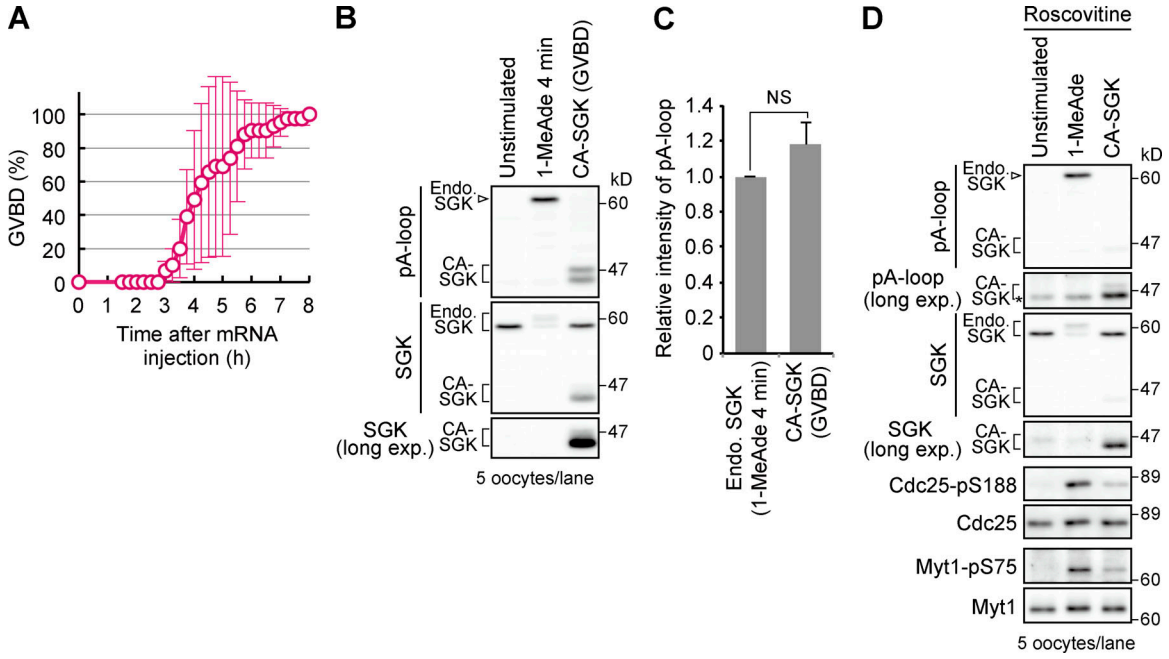

Figure 5. **SGK is sufficient for the meiotic G2/M transition. (A–C)** CA-SGK expression induces the meiotic G2/M transition. Unstimulated oocytes were injected with mRNA encoding CA-SGK. GVBD was monitored every 15 min during incubation. The graph shows percentage of oocytes that had undergone GVBD by the indicated time points (A; mean ± SD from three independent experiments). CA-SGK–expressing oocytes at GVBD, unstimulated oocytes, and 1-MeAde–treated oocytes were analyzed by immunoblotting (B). Phosphorylation levels of the A-loop of endogenous SGK in 1-MeAde–treated oocytes and CA-SGK at GVBD were quantitated from the immunoblots in B. The graph shows relative phosphorylation levels (C; mean ± SD from three independent experiments). NS, P = 0.06 (one-tailed *t* test). **(D)** CA-SGK expression induces regulatory phosphorylation of Cdc25 and Myt1 to trigger cyclin B–Cdk1 activation. Unstimulated oocytes were treated with 1-MeAde for 4 min in the presence of roscovitine. For expression of CA-SGK, unstimulated oocytes were injected with the mRNA, incubated with roscovitine, collected at the time point at which 50% of CA-SGK–expressing oocytes exhibited GVBD in the absence of roscovitine (5 h 45 min in this sampling), and analyzed by immunoblotting. Note that in the immunoblot of phospho-A-loop after a long exposure (pA-loop, long exp.), weak nonspecific bands were detected at almost the same size as CA-SGK (asterisk). The data are representative of two independent experiments. Full blots for B and D are presented in Fig. S8.

knowledge, this is the first report that SGK is involved in M-phase entry.

In parallel with the present study, Hosoda et al. (2019) showed that SGK is required for the increase in intracellular pH after 1-MeAde stimulation in starfish oocytes. They suggested that the pH increase is not required for cyclin B–Cdk1 activation but is required for processes after GVBD in ovarian oocytes. The functions of SGK have been mainly studied in mammalian cells, which express three SGK isoforms: SGK1, SGK2, and SGK3 (Pearce et al., 2010). Although mammalian SGKs are reportedly involved in various processes, such as cell survival and tumorigenesis, in somatic cells (Lang et al., 2006; Bruhn et al., 2013), their functions in germ cells remain unclear. To the best of our knowledge, studies presented here and by Hosoda et al. (2019) are the first indication of the functions of SGK in germ cells.

Among the mammalian SGK isoforms, only SGK3 contains an N-terminal PX domain (Liu et al., 2000; Pearce et al., 2010). sfSGK also has a PX domain and is therefore likely an orthologue of mammalian SGK3 (Hosoda et al., 2019). The PX domain of mammalian SGK3 binds to phosphatidylinositol 3-phosphate (PI-3P), which is a phosphorylated derivative of phosphatidylinositol at the 3-position of the inositol ring (Virbasius et al., 2001). This interaction is essential for the localization and activation of SGK3 (Virbasius et al., 2001; Lien et al., 2017). PI-3P is generated by dephosphorylation of PI-345P_3 at the 4- and 5-positions of the inositol ring (Lien et al., 2017). PI3K, which produces PI-345P_3 from phosphatidylinositol 4,5-bisphosphate, is activated downstream of receptor tyrosine kinases and GPCRs (Vanhaesebroeck et al., 2010). Thus, production of PI-3P from PI-345P_3 may occur downstream of these receptors. Indeed, a recent report suggested that this mechanism is implicated in activation of SGK3 after stimulation by IGF-1, an agonist for a receptor tyrosine kinase (Malik et al., 2018). In this context, SHIP2 and INPP4A/B are proposed to be phosphatases for PI-3P production, although the regulatory mechanisms remain elusive (Malik et al., 2018). Furthermore, it is unclear whether PI-345P_3 is a source of PI-3P for SGK activation in GPCR-dependent signaling. We previously showed that PI-345P_3 is generated on the plasma membrane after 1-MeAde stimulation in starfish oocytes (Hiraoka et al., 2016). This PI-345P_3 may be metabolized to PI-3P for SGK activation. Our present results suggest that the atypical Gβγ pathway cooperates with PI3K to activate sfSGK (Fig. 6). Thus, we propose that the atypical Gβγ pathway activates phosphatases that produce PI-3P from PI-345P_3 downstream of GPCR.

Another mechanism for PI-3P production is phosphorylation of phosphatidylinositol at the 3-position, which occurs on early endosomes during intracellular vesicle trafficking and endocytosis (Vanhaesebroeck et al., 2010; Lien et al., 2017). GPCRs are

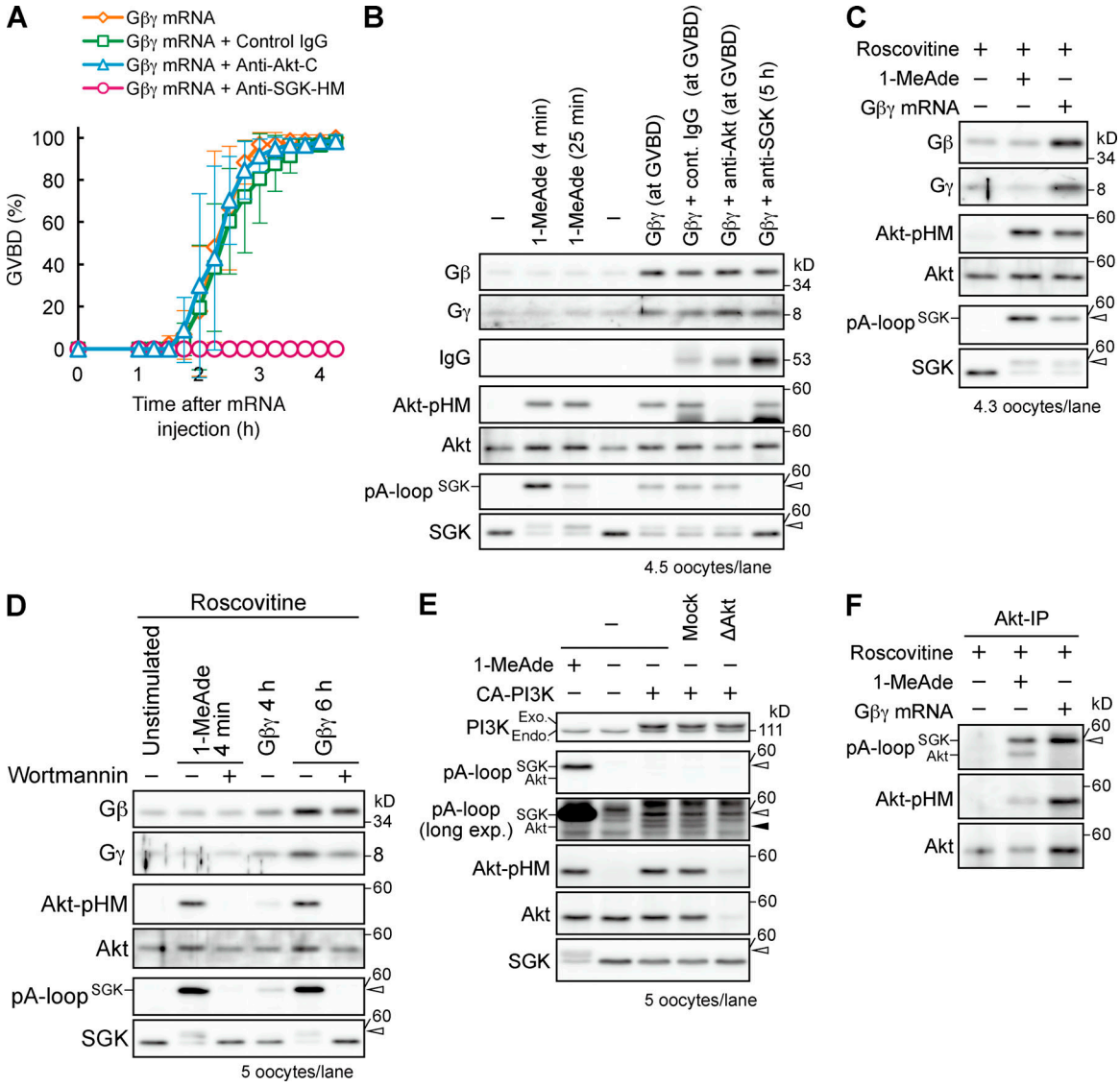

Figure 6. **SGK is activated by cooperation of the Gβγ-PI3K and atypical Gβγ pathways. (A and B)** Exogenous expression of Gβγ induces the meiotic G2/M transition in a SGK-dependent manner. Unstimulated oocytes were injected with the indicated antibodies and subsequently injected with mRNA encoding Gβγ. Thereafter, GVBD was monitored (A; mean ± SD from three independent experiments). Oocytes were collected when GVBD occurred. Anti-sfSGK-HM antibody–injected oocytes, which did not undergo GVBD, were collected 5 h after mRNA injection. For 1-MeAde treatment, unstimulated oocytes were treated with 1-MeAde for 4 or 25 min (GVBD occurred at ∼21 min) and then analyzed by immunoblotting (B). **(C)** Exogenous Gβγ expression induces SGK activation. Unstimulated oocytes were treated with 1-MeAde for 4 min in the presence of roscovitine or injected with mRNA encoding Gβγ and then incubated with roscovitine for 6 h. Thereafter, extracts were prepared from these oocytes and analyzed by immunoblotting. **(D)** Gβγ-induced SGK activation requires PI3K. Unstimulated oocytes were treated with 1-MeAde or injected with mRNA encoding Gβγ, incubated in the presence of roscovitine with or without wortmannin, and analyzed by immunoblotting. **(E)** PI3K is not sufficient for activation of SGK. Unstimulated oocytes were treated with 1-MeAde for 4 min or injected with mRNA encoding CA-PI3K and incubated for 3 h. Extracts of CA-PI3K–expressing oocytes were immunodepleted using control IgG (Mock) or the anti-sfAkt-C antibody (ΔAkt) and analyzed by immunoblotting. A closed arrowhead in the blot of pA-loop indicates the position of Akt. **(F)** Expression of exogenous Gβγ fails to induce A-loop phosphorylation of Akt. Endogenous Akt was immunoprecipitated (IP) from the extracts in C and analyzed by immunoblotting. Open arrowheads in B–F indicate the position of active SGK. The data are representative of two independent experiments in B, D, and E and three independent experiments in C and F. Full blots for B–F are presented in Fig. S8.

frequently endocytosed after agonist stimulation (Tsao and von Zastrow, 2001). Thus, endocytosis may be induced by 1-MeAde stimulation and contribute to activation of SGK in starfish oocytes. Many aspects of these scenarios, such as the dynamics of PI-3P and the molecular identity of the atypical Gβγ pathway, remain unclear. Nonetheless, these working models could be tested in future studies and may help to elucidate the regulatory mechanisms of not only sfSGK but also mammalian SGK3 in somatic cells.

Our present results showed that the contribution of Akt to the trigger was, if any, undetectable (Figs. 2 and S2) and that this was probably due to its weak activation (Fig. S4). This was inconsistent with our previous study showing that Akt is necessary for the meiotic G2/M transition (Okumura et al., 2002). In

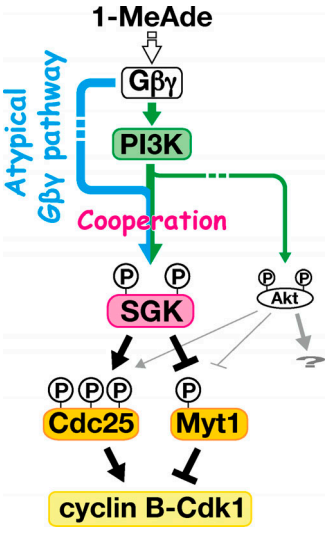

Figure 7. **SGK triggers cyclin B–Cdk1 activation in 1-MeAde signaling.** Downstream of 1-MeAde stimulation, Gβγ activates the PI3K pathway (green arrow) and the atypical Gβγ pathway (cyan arrow). SGK is activated by cooperation of these pathways and subsequently activates and inactivates Cdc25 and Myt1, respectively, via direct phosphorylation. Consequently, reversal of the balance of Cdc25 and Myt1 activities triggers cyclin B–Cdk1 activation. Akt is weakly activated after 1-MeAde stimulation and may phosphorylate Cdc25 and Myt1 at undetectable levels. However, Akt is dispensable for cyclin B–Cdk1 activation and may have other functions in oocytes.

the previous study, in addition to the antibody, we also used competitive peptides derived from the A-loop or HM of Akt to inhibit Akt activation. Akt and SGK have common upstream kinases; therefore, peptide competition likely inhibited activation of both Akt and SGK. In the present study, successful generation of anti-phospho-A-loop, anti-sfSGK-HM, and anti-sfAkt-HM antibodies enabled us to evaluate the specificities of the neutralizing antibodies more precisely. In addition, Akt was dispensable at least in all cases tested in the current study, which used oocytes isolated from seven starfish collected in three different areas in Japan. Thus, our current conclusions are more convincing than our previous ones. The role of Akt may be independent of the trigger. However, Akt has the potential to trigger cyclin B–Cdk1 activation (Okumura et al., 2002). Indeed, overexpression of the constitutively active form of Akt (40-fold higher than the endogenous Akt level) induces the meiotic G2/M transition (Okumura et al., 2002; Hiraoka et al., 2016). Furthermore, the regulatory effects of phosphorylation of the Akt/SGK consensus motifs on Myt1 and Cdc25 activities were originally demonstrated using Akt as a kinase in in vitro experiments (Okumura et al., 2002; Hiraoka et al., 2016). Therefore, if there are a limited number of unknown circumstances in which Akt is strongly activated and/or highly expressed in oocytes, Akt may significantly contribute to the trigger by functioning as a redundant kinase with SGK. Such situations may arise depending on age, the breeding season, and environmental factors, such as temperature and the type and availability of food. We have used wild animals, whose living environment potentially varied. This may also explain the discrepancy in the requirement for Akt. It would be intriguing to investigate how the expression and activation levels of Akt and SGK are regulated during oogenesis.

We made some interesting observations regarding activation of Akt that depends on the binding of PI-345P_3 to its pleckstrin homology domain (Bruhn et al., 2013). Expression of CA-PI3K, but not of Gβγ, induced A-loop phosphorylation of Akt (Fig. 6, E and F). We previously reported that CA-PI3K induces a higher level of PI-345P_3 than those produced upon 1-MeAde stimulation or Gβγ expression (Hiraoka et al., 2016). Thus, it is possible that a high level of PI-345P_3 alone can induce Akt activation, whereas a low level of PI-345P_3 requires an additional mechanism to enhance A-loop phosphorylation.

In summary, we identified SGK as the trigger kinase for activation of cyclin B–Cdk1 at M-phase entry and as the target of the collaborative actions of PI3K and the atypical Gβγ pathway. These findings not only demonstrate the novel role of SGK in the triggering of M-phase but also provide insights into the regulatory mechanisms of SGK activation, particularly with regard to PI-3P production.

Materials and methods

Chemicals

Roscovitine (Calbiochem), wortmannin (LC Laboratories), and BX795 (Enzo Life Sciences) were dissolved in DMSO at concentrations of 50, 20, and 6 mM, respectively, as stock solutions and used at final concentrations of 45, 40, and 6 µM, respectively.

DNA constructs

For CA-SGK, an N-terminal fragment of sfSGK containing the PX domain (Met1-Asp132) was substituted with a myristoylation sequence (MGSSKSKPKDPSQR) by PCR. Thereafter, the insert was cloned into a modified pSP64-S vector, in which the SP6 promoter for in vitro transcription had been substituted by a T7 promoter sequence (Terasaki et al., 2003; Hiraoka et al., 2016), using an In-Fusion kit (Takara Bio). Finally, Thr479 in the HM was substituted with Glu by PCR, and the point mutation was verified by sequencing. Constructs encoding untagged sfAkt, CA-PI3K in which Flag tag (DYKDDDDKLE) and plasma membrane–targeting sequence including a CAAX motif (KMSKDGKKKKKKSKTKCVIM) were fused to the N- and C-terminus of the p110 catalytic subunit of sfPI3K, respectively; untagged sfGβ; and untagged sfGγ for mRNA preparation were prepared as described previously (Hiraoka et al., 2016).

Preparation of recombinant proteins

Recombinant sfMyt1 (N229A for the kinase-dead mutant or S75A mutant) cloned into the pGEX-4T-1 vector was expressed in *Escherichia coli* strain BL21 (DE3; Invitrogen) as an N-terminal GST-tagged protein, purified using glutathione-Sepharose 4B beads (GE Healthcare), and dialyzed against storage buffer (20 mM Pipes, pH 6.8, 200 mM sucrose, and 1 mM DTT). For His_6-Cdc25 (WT or S188A mutant), *E. coli* strain BL21 (DE3) was transformed with the pET21a construct. Expressed His_6-Cdc25 were purified from inclusion bodies under denaturing conditions (6 M urea) using Probond-Resin (Invitrogen) and then refolded via stepwise reduction of the urea concentration by

dialysis using EasySep (TOMY) for 2 h against TBS (50 mM Tris and 150 mM NaCl, pH 7.5) containing 4 M urea, for 2 h against TBS containing 2 M urea, and for 2 h against TBS lacking urea. To prepare the recombinant GST-fused peptide substrates (AS peptide, AGRPRAATFIESG; sfMyt1-S75 peptide, ESRPRAVSFRQSE; sfCdc25-S188 peptide, AGRPRQISFIESG), *E. coli* strain BL21-CodonPlus-RIL (Agilent Technologies) was transformed with the pGEX-4T-1 constructs. The expressed GST-peptides were purified using glutathione-Sepharose 4B and dialyzed against PBS (137 mM NaCl, 2.68 mM KCl, 10 mM Na_2HPO_4, and 1.76 mM KH_2PO_4, pH 7.4). A recombinant C-terminal 88-aa fragment of sfAkt was prepared as previously described (Okumura et al., 2002).

Antibody generation

Antibodies were generated by immunizing rabbits (Biologica) and then purified using antigens. Antigens used for immunization and antibody purification were a phospho-peptide of the A-loop of sfAkt (Lys304–Pro320, phosphorylated at Thr315) for the anti-phospho-A-loop antibody, a C-terminal 17-aa peptide of sfSGK (Ser473–Asp489) for the anti-sfSGK-HM antibody (Hosoda et al., 2019), a C-terminal 88-aa fragment of sfAkt (Leu399–Leu486) for the anti-sfAkt-C antibody, and a C-terminal 16-aa peptide of sfAkt (Pro471–Leu486) for the anti-sfAkt-HM antibody. Control IgG for microinjection or immunoprecipitation was purified from rabbit preimmune serum using protein A–Sepharose 4B (Sigma-Aldrich).

Oocyte preparation

Starfish *Asterina pectinifera* (renamed *Patiria pectinifera* in the 2007 National Center for Biotechnology Information Taxonomy Browser) was collected during the breeding season and kept in laboratory aquaria supplied with circulating seawater at 14°C. Fully grown unstimulated oocytes with follicle cells were manually isolated from ovaries using forceps. Thereafter, the follicle cells were removed by washing oocytes with calcium-free artificial seawater (476 mM NaCl, 10 mM KCl, 36 mM $MgCl_2$, 18 mM $MgSO_4$, and 20 mM H_3BO_3, pH 8.2). All treatments with 1-MeAde or other chemicals, as well as microinjections, were performed in artificial seawater (ASW: 462 mM NaCl, 9 mM $CaCl_2$, 10 mM KCl, 36 mM $MgCl_2$, 18 mM $MgSO_4$, and 20 mM H_3BO_3, pH 8.2) at 23°C. Oocytes were stimulated with 0.5 µM 1-MeAde.

Immunoblotting

Oocytes were lysed by vortexing in Laemmli sample buffer (LSB) and then heated at 95°C for 5 min. Proteins were separated by SDS-PAGE (Laemmli, 1970) on an 8% or 8.5% gel (separating gel: 8% or 8.5% acrylamide, 0.22% or 0.23% *N*,*N*′-methylenebisacrylamide, 375 mM Tris, 0.1% SDS, 0.1% APS, and 0.1% tetramethylethylenediamine [TEMED], pH 8.8; stacking gel: 3.6% acrylamide, 0.096% *N*,*N*′-methylenebisacrylamide, 120 mM Tris, 0.1% SDS, 0.2% APS, and 0.1% TEMED, pH 6.8; and electrophoresis buffer: 25 mM Tris, 192 mM glycine, and 0.1% SDS) and transferred to a polyvinylidene fluoride (PVDF) membrane (Millipore; Towbin et al., 1979) using transfer buffer (100 mM Tris, 192 mM glycine, 0.1% SDS, and 20% methanol). Phos-tag SDS-PAGE was performed in accordance with the manufacturer's protocol using an 8% polyacrylamide gel containing 4 µM Phos-tag (Fujifilm) and 8 µM $MnCl_2$. A modified 15% gel and buffer were used to detect Gγ (separating gel: 15% acrylamide, 0.41% *N*,*N*′-methylenebisacrylamide, 750 mM Tris, 0.1% SDS, 0.1% APS, and 0.1% TEMED, pH 8.8; stacking gel: 3.6% acrylamide, 0.096% *N*,*N*′-methylenebisacrylamide, 240 mM Tris, 0.1% SDS, 0.2% APS, and 0.1% TEMED, pH 6.8; and electrophoresis buffer: 50 mM Tris, 384 mM glycine, and 0.1% SDS). The membranes were then blocked by incubation in blocking buffer (5% skimmed milk prepared in TBS containing 0.1% Tween-20 [TBS-T]) for 1 h for the anti-sfMyt1 phospho-Ser75, anti-sfMyt1, and anti-GST antibodies, but not for the other antibodies. The primary antibodies were anti-phospho-A-loop (rabbit purified polyclonal antibody, 1:50 in TBS-T), anti-sfAkt-C (rabbit purified polyclonal antibody, 1:1,000 in Can Get Signal Solution 1), anti-sfAkt-HM-rabbit #1 (rabbit purified polyclonal antibody, 1:20 in TBS-T), anti-sfAkt-HM-rabbit #2 (rabbit purified polyclonal antibody, 1:20 in TBS-T), anti-sfAkt phospho-Ser477 (Hiraoka et al., 2011; antigen, QFEKFpSYSGDK; rabbit purified polyclonal antibody, 1:1,000 in Can Get Signal Solution 1), anti-sfSGK-HM (rabbit purified polyclonal antibody, 1:2,000 in Can Get Signal Solution 1), anti-sfCdc25 phospho-Ser188 (Hiraoka et al., 2016; antigen, GRPRQIpSFIESG; rabbit polyclonal antiserum, 1:1,000 in Can Get Signal Solution 1), anti-sfCdc25 (Okumura et al., 1996; antigen, C-terminal 153-aa fragment; rabbit polyclonal antiserum, 1:2,000 in Can Get Signal Solution 1), anti-Cdk1 phospho-Tyr15 (Cell Signaling Technology; #9111s, rabbit purified polyclonal antibody, 1:1,000 in Can Get Signal Solution 1), anti-PSTAIR to detect Cdk1 (a gift from M. Yamashita and T. Nagahama, National Institute for Basic Biology, Okazaki, Japan; mouse monoclonal antibody, 1:50,000 in Can Get Signal Solution 1), anti-sfMyt1 phospho-Ser75 (Hiraoka et al., 2016; antigen, RPRAVpSFRQ; rabbit purified polyclonal antibody, 1:100 in blocking buffer), anti-sfMyt1 (Okumura et al., 2002; antigen, 124-aa N-terminal fragment; rabbit purified polyclonal antibody, 1:200 in TBS-T), anti-GST (GE Healthcare; 1:500 in blocking buffer), anti-pan-phospho-Akt/SGK substrate (Cell Signaling Technology; #9611s, rabbit purified polyclonal antibody, 1:1,000 in Can Get Signal Solution 1), anti-starfish p110β to detect sfPI3K (Hiraoka et al., 2016; antigen, full-length starfish p110β; rabbit purified polyclonal antibody, 1:1,000 in Can Get Signal Solution 1), anti-sfGβ (Hiraoka et al., 2016; antigen, full-length sfGβ; rabbit polyclonal antiserum, 1:1,000 in Can Get Signal Solution 1), and anti-sfGγ (Hiraoka et al., 2016; antigen, 16-aa N-terminal peptide; rabbit purified polyclonal antibody, 1:100 in Can Get Signal Solution 1). HRP-conjugated secondary antibodies were anti-goat IgG (Sigma-Aldrich; #A5420, rabbit purified polyclonal antibody, 1:500 in blocking buffer for anti-GST antibody), anti-mouse IgG (Dako; #P0260, rabbit purified polyclonal antibody, 1:2,000 in Can Get Signal Solution 2 for anti-PSTAIR antibody), and anti-rabbit IgG (GE Healthcare; #NA9340V, 1:2,000 in TBS-T for anti-phospho-A-loop, anti-sfAkt-HM-rabbit #1, anti-sfAkt-HM-rabbit #2, anti-sfSGK-HM, anti-sfMyt1 phospho-Ser75, and anti-pan-phospho-Akt/SGK substrate antibodies; in blocking buffer for the anti-sfMyt1

antibody; and in Can Get Signal Solution 2 for the other antibodies). When the signal derived from IgG heavy chains hampered detection, TrueBlot (Rockland; #18-8816-33, 1:2,000 in Can Get Signal Solution 2) was used instead of the secondary antibody. Signals were visualized with ECL Prime (GE Healthcare), and digital images were acquired on a LAS4000 mini imager (Fujifilm). Quantitation was performed using ImageJ (National Institutes of Health). Graphs were generated using Microsoft Excel. Brightness and contrast were adjusted using ImageJ.

Microinjection

Microinjection was performed as described previously (Kishimoto, 1986). mRNAs for exogenous protein expression in starfish oocytes were transcribed from pSP64-S constructs using a mMESSAGE mMACHINE kit (Ambion), dissolved in water, and injected into unstimulated oocytes (20 pg for sfAkt, 20 pg for CA-SGK, and 40 pg for CA-PI3K). To express starfish Gβγ, 50 pg of an equimolar mixture of mRNAs encoding sfGβ and sfGγ was injected. The incubation time for protein expression was determined based on the amount of time taken to induce GVBD or HM phosphorylation of Akt to a comparable extent as that induced by 1-MeAde. For microinjection of antibodies, concentration of antibodies and buffer exchange with PBS were performed using a 50K cutoff Amicon Ultra filter (Millipore). NP-40 was added at a final concentration of 0.05%. Unstimulated oocytes were injected with 230 pg of the anti-TOR antibody, 85 pg of the anti-sfAkt-C, 24 pg of the anti-sfAkt-HM (rabbit #1), 30 pg of the anti-sfAkt-HM (rabbit #2), or 200 pg of the anti-sfSGK-HM antibody. 1-MeAde was added after incubation for 1 h.

Immunoprecipitation and immunodepletion

To prepare antibody-bound beads, antibodies (anti-sfAkt-C antibody, 2.5 µg/µl beads, 0.83 µg for 10 oocytes; and anti-sfSGK-HM antibody, 2 µg/µl beads, 2.7 µg for 10 oocytes) were incubated with protein A–Sepharose (Sigma-Aldrich) for >2 h on ice. Antibody-bound beads were washed with TBS and lysis buffer (80 mM β-glycerophosphate, 20 mM EGTA, 10 mM MOPS, pH 7.0, 100 mM sucrose, 100 mM KCl, 1 mM DTT, 1× cOmplete EDTA-free [Merck], 0.5 mM sodium orthovanadate, 1 µM okadaic acid [Calbiochem], and 0.5% NP-40) and used for immunoprecipitation. For cross-linking, antibody-bound beads were washed with TBS and borate buffer (0.2 M NaCl and 0.2 M boric acid, pH 9.0) and then incubated with 3.75 mM disuccinimidyl suberate prepared in borate buffer at 24°C for 30 min. Thereafter, the supernatant was discarded, and the beads were further incubated in 1 M ethanolamine (pH 8.0) at 24°C for 15 min and finally washed with TBS and lysis buffer. For immunoprecipitation, freeze-thawed oocytes in ASW (10 oocytes/µl of ASW for immunoprecipitation of Akt and SGK) were lysed by adding six volumes of lysis buffer and incubating samples on ice for 30 min, followed by gentle vortexing. Lysates were centrifuged at 20,000 *g* at 4°C for 15 min. The supernatant represented the oocyte extract. Antibody-bound beads were incubated with the oocyte extract (60 oocytes for immunoprecipitation of Akt, 30 oocytes for depletion of Akt, and 15 oocytes for immunoprecipitation and depletion of SGK) for 90 min on ice, separated from flow-through extracts, and washed with lysis buffer. For immunoprecipitation of Akt from oocytes that had been injected with the anti-sfSGK-HM antibody, extracts were preincubated with protein A–Sepharose 4B to remove injected IgG. LSB was added to the input extracts, flow-through extracts, and beads for immunoblot analysis. All samples were then heated at 95°C for 5 min and subjected to SDS-PAGE. To prepare mock, Akt-depleted, and SGK-depleted extracts for the kinase assay, freeze-thawed oocytes in ASW (5 oocytes/µl of ASW) were lysed by adding 6.5 volumes of lysis buffer. The extract was then prepared as described above and mixed with beads bound to control IgG, the anti-sfAkt-C antibody, or the anti-sfSGK-HM antibody. After incubation at 4°C for 45 min, the supernatant was analyzed by immunoblotting or used for the kinase assay with peptide substrates.

In vitro phosphorylation of sfCdc25 and sfMyt1

Recombinant sfCdc25 (final concentration of 5 ng/µl) or sfMyt1 (final concentration of 200 ng/µl) was incubated with N-terminal GST-tagged hSGK3 (final concentration of 10 ng/µl; SignalChem) in reaction buffer (80 mM β-glycerophosphate, 20 mM EGTA, 1 mM MOPS, pH 7.0, 1 mM DTT, 1 mM ATP, 5 mM $MgCl_2$, and 0.3% NP-40) at 30°C for 50 min. The reaction was stopped by adding LSB followed by heating at 95°C for 5 min. Samples were analyzed by immunoblotting with phospho-specific antibodies.

GST-peptide kinase assay

Freeze-thawed oocytes in ASW (5 oocytes/µl of ASW) were lysed by adding 6.5 volumes of lysis buffer and then incubating samples on ice for 30 min, followed by gentle vortexing. Lysates were centrifuged at 20,000 *g* at 4°C for 15 min. The supernatant was used for the kinase assay. Mock, Akt-depleted, and SGK-depleted extracts were prepared as described above. For the kinase assay, a reaction mixture containing the GST-AS peptide as a substrate (80 mM β-glycerophosphate, 15 mM $MgCl_2$, 20 mM EGTA, 10 mM MOPS, pH 7.0, 1 mM DTT, 1× cOmplete EDTA-free, 2 mM ATP, 0.5 mM sodium orthovanadate, 1 µM okadaic acid, 0.1 mg/ml GST-peptide, and 0.3% NP-40) was added to an equal volume of the extract. After incubation at 30°C, the reaction solution was mixed with LSB, heated at 95°C for 5 min, and then analyzed by immunoblotting with the anti-pan-phospho-Akt/SGK substrate antibody.

Dot blot

Unphosphorylated and phosphorylated (at PDK1 site) peptides derived from A-loop of sfAkt or sfSGK were synthesized by manufacturers (Biologica, purity >95%; CKEDLSYGNTTSTFCGTPE and CKEDLSYGNTTSpTFCGTPE for sfAkt; CKEGIAAKGTTSTFCGTPE and CKEGIAAKGTTSpTFCGTPE for sfSGK). These peptides were dissolved in water, and the concentration was confirmed by Protein Quantification Kit-Rapid (Dojindo Molecular Technologies). A dilution series was prepared by diluting 0.1 µM of the peptide with water. PVDF membrane was immersed in methanol, and subsequently in water. The membrane was put on parafilm. Then, 1 µl of each 0.1-µM or diluted peptide solution was spotted on the membrane. After drying, the membrane were immersed in methanol, subsequently in TBS-T, and then treated with the anti-phospho-A-loop antibody as described in Immunoblotting.

Statistical analysis

Statistical significance was calculated using the unpaired one-tailed Student's *t* test in Microsoft Excel with StatPlus (AnalystSoft). Statistical significance was defined as $P < 0.05$. In the calculation, data distribution was assumed to be normal but this was not formally tested.

Accession numbers

GenBank accession numbers are as follows: LC430700 for sfSGK, AB076395 for sfCdc25, AB060280 for sfMyt1, AB060291 for sfAkt, LC017891 for sfGβ, LC017892 for sfGγ, and LC017893 for the sfPI3K catalytic subunit p110β.

Online supplemental material

Fig. S1 shows an alignment of amino acid sequences of sfAkt and sfSGK to provide the region of the antigens and a dot blot to evaluate sensitivity of the anti-phospho-A-loop antibody to sfAkt and sfSGK. Fig. S2 shows inhibition of Akt by newly generated anti-sfAkt-HM antibodies. Fig. S3 shows kinase assays using oocyte extracts with GST-peptide substrates derived from sfCdc25 and sfMyt1. Fig. S4 provides detailed description and data about comparison of total activities and amounts of active forms between endogenous SGK and endogenous Akt. Figs. S5, S6, S7, S8, S9, and S10 provide full blots used in Figs. 1, 2, 3, 4, 5, and 6.

Acknowledgments

We thank E. Okumura (Tokyo Institute of Technology, Yokohama, Japan) for helpful discussions, suggestions, and providing recombinant Cdc25 and Myt1, as well as M. Terasaki (UConn Health, Farmington, CT) for providing the pSP64-S vector.

This work was supported by grants-in-aid to T. Kishimoto from the Japan Society for the Promotion of Science (grants 25291043 and 16H04783) and Takeda Science Foundation.

The authors declare no competing financial interests.

Author contributions: conceptualization, D. Hiraoka and T. Kishimoto; data curation, D. Hiraoka; formal analysis, D. Hiraoka; funding acquisition, T. Kishimoto; investigation, D. Hiraoka and E. Hosoda; methodology, D. Hiraoka; project administration, D. Hiraoka and T. Kishimoto; resources, D. Hiraoka, E. Hosoda, K. Chiba, and T. Kisimoto; supervision, T. Kishimoto; validation, D. Hiraoka and E. Hosoda; visualization, D. Hiraoka and T. Kishimoto; writing (original draft), D. Hiraoka; writing (review and editing), D. Hiraoka, E. Hosoda, K. Chiba, and T. Kishimoto.

Submitted: 20 December 2018
Revised: 3 June 2019
Accepted: 26 July 2019

References

Abe, Y., E. Okumura, T. Hosoya, T. Hirota, and T. Kishimoto. 2010. A single starfish Aurora kinase performs the combined functions of Aurora-A and Aurora-B in human cells. *J. Cell Sci.* 123:3978–3988. https://doi.org/10.1242/jcs.076315

Adhikari, D., and K. Liu. 2014. The regulation of maturation promoting factor during prophase I arrest and meiotic entry in mammalian oocytes. *Mol. Cell. Endocrinol.* 382:480–487. https://doi.org/10.1016/j.mce.2013.07.027

Bruhn, M.A., R.B. Pearson, R.D. Hannan, and K.E. Sheppard. 2013. AKT-independent PI3-K signaling in cancer - emerging role for SGK3. *Cancer Manag. Res.* 5:281–292.

Chiba, K., K. Kontani, H. Tadenuma, T. Katada, and M. Hoshi. 1993. Induction of starfish oocyte maturation by the β γ subunit of starfish G protein and possible existence of the subsequent effector in cytoplasm. *Mol. Biol. Cell.* 4:1027–1034. https://doi.org/10.1091/mbc.4.10.1027

Dorée, M. 1982. Protein synthesis is not involved in initiation or amplification of the maturation-promoting factor (MPF) in starfish oocytes. *Exp. Cell Res.* 139:127–133. https://doi.org/10.1016/0014-4827(82)90326-3

Dunphy, W.G., and J.W. Newport. 1988. Unraveling of mitotic control mechanisms. *Cell.* 55:925–928. https://doi.org/10.1016/0092-8674(88)90234-6

Dupré, A., E.M. Daldello, A.C. Nairn, C. Jessus, and O. Haccard. 2014. Phosphorylation of ARPP19 by protein kinase A prevents meiosis resumption in *Xenopus* oocytes. *Nat. Commun.* 5:3318. https://doi.org/10.1038/ncomms4318

Gaffré, M., A. Martoriati, N. Belhachemi, J.P. Chambon, E. Houliston, C. Jessus, and A. Karaiskou. 2011. A critical balance between Cyclin B synthesis and Myt1 activity controls meiosis entry in *Xenopus* oocytes. *Development.* 138:3735–3744. https://doi.org/10.1242/dev.063974

García-Martínez, J.M., and D.R. Alessi. 2008. mTOR complex 2 (mTORC2) controls hydrophobic motif phosphorylation and activation of serum- and glucocorticoid-induced protein kinase 1 (SGK1). *Biochem. J.* 416:375–385. https://doi.org/10.1042/BJ20081668

Gheghiani, L., D. Loew, B. Lombard, J. Mansfeld, and O. Gavet. 2017. PLK1 activation in late G2 sets up commitment to mitosis. *Cell Reports.* 19:2060–2073. https://doi.org/10.1016/j.celrep.2017.05.031

Haccard, O., and C. Jessus. 2006a. Oocyte maturation, Mos and cyclins--a matter of synthesis: two functionally redundant ways to induce meiotic maturation. *Cell Cycle.* 5:1152–1159. https://doi.org/10.4161/cc.5.11.2800

Haccard, O., and C. Jessus. 2006b. Redundant pathways for Cdc2 activation in *Xenopus* oocyte: either cyclin B or Mos synthesis. *EMBO Rep.* 7:321–325. https://doi.org/10.1038/sj.embor.7400611

Hégarat, N., S. Rata, and H. Hochegger. 2016. Bistability of mitotic entry and exit switches during open mitosis in mammalian cells. *BioEssays.* 38:627–643. https://doi.org/10.1002/bies.201600057

Hiraoka, D., S. Hori-Oshima, T. Fukuhara, K. Tachibana, E. Okumura, and T. Kishimoto. 2004. PDK1 is required for the hormonal signaling pathway leading to meiotic resumption in starfish oocytes. *Dev. Biol.* 276:330–336. https://doi.org/10.1016/j.ydbio.2004.08.036

Hiraoka, D., E. Okumura, and T. Kishimoto. 2011. Turn motif phosphorylation negatively regulates activation loop phosphorylation in Akt. *Oncogene.* 30:4487–4497. https://doi.org/10.1038/onc.2011.155

Hiraoka, D., R. Aono, S. Hanada, E. Okumura, and T. Kishimoto. 2016. Two new competing pathways establish the threshold for cyclin-B-Cdk1 activation at the meiotic G2/M transition. *J. Cell Sci.* 129:3153–3166. https://doi.org/10.1242/jcs.182170

Hosoda, E., D. Hiraoka, N. Hirohashi, S. Omi, T. Kishimoto, and K. Chiba. 2019. SGK regulates pH increase and cyclin B-Cdk1 activation to resume meiosis in starfish ovarian oocytes. *J. Cell Biol.* https://doi.org/10.1083/jcb.201812133

Hunt, T. 1989. Maturation promoting factor, cyclin and the control of M-phase. *Curr. Opin. Cell Biol.* 1:268–274. https://doi.org/10.1016/0955-0674(89)90099-9

Jaffe, L.A., and J.R. Egbert. 2017. Regulation of mammalian oocyte meiosis by intercellular communication within the ovarian follicle. *Annu. Rev. Physiol.* 79:237–260. https://doi.org/10.1146/annurev-physiol-022516-034102

Jaffe, L.A., C.J. Gallo, R.H. Lee, Y.K. Ho, and T.L. Jones. 1993. Oocyte maturation in starfish is mediated by the β γ-subunit complex of a G-protein. *J. Cell Biol.* 121:775–783. https://doi.org/10.1083/jcb.121.4.775

Kanatani, H., and Y. Hiramoto. 1970. Site of action of 1-methyladenine in inducing oocyte maturation in starfish. *Exp. Cell Res.* 61:280–284. https://doi.org/10.1016/0014-4827(70)90448-9

Kanatani, H., H. Shirai, K. Nakanishi, and T. Kurokawa. 1969. Isolation and indentification on meiosis inducing substance in starfish Asterias amurensis. *Nature.* 221:273–274. https://doi.org/10.1038/221273a0

Kishimoto, T. 1986. Microinjection and cytoplasmic transfer in starfish oocytes. *Methods Cell Biol.* 27:379–394. https://doi.org/10.1016/S0091-679X(08)60359-3

Kishimoto, T. 2003. Cell-cycle control during meiotic maturation. *Curr. Opin. Cell Biol.* 15:654–663. https://doi.org/10.1016/j.ceb.2003.10.010

Kishimoto, T. 2015. Entry into mitosis: a solution to the decades-long enigma of MPF. *Chromosoma.* 124:417–428. https://doi.org/10.1007/s00412-015-0508-y

Kishimoto, T. 2018. MPF-based meiotic cell cycle control: Half a century of lessons from starfish oocytes. *Proc. Jpn. Acad., Ser. B, Phys. Biol. Sci.* 94: 180–203. https://doi.org/10.2183/pjab.94.013

Kobayashi, T., and P. Cohen. 1999. Activation of serum- and glucocorticoid-regulated protein kinase by agonists that activate phosphatidylinositide 3-kinase is mediated by 3-phosphoinositide-dependent protein kinase-1 (PDK1) and PDK2. *Biochem. J.* 339:319–328. https://doi.org/10.1042/bj3390319

Kobayashi, H., J. Minshull, C. Ford, R. Golsteyn, R. Poon, and T. Hunt. 1991. On the synthesis and destruction of A- and B-type cyclins during oogenesis and meiotic maturation in *Xenopus laevis*. *J. Cell Biol.* 114:755–765. https://doi.org/10.1083/jcb.114.4.755

Komrskova, P., A. Susor, R. Malik, B. Prochazkova, L. Liskova, J. Supolikova, S. Hladky, and M. Kubelka. 2014. Aurora kinase A is not involved in CPEB1 phosphorylation and cyclin B1 mRNA polyadenylation during meiotic maturation of porcine oocytes. *PLoS One.* 9:e101222. https://doi.org/10.1371/journal.pone.0101222

Laemmli, U.K. 1970. Cleavage of structural proteins during the assembly of the head of bacteriophage T4. *Nature.* 227:680–685. https://doi.org/10.1038/227680a0

Lang, F., C. Böhmer, M. Palmada, G. Seebohm, N. Strutz-Seebohm, and V. Vallon. 2006. (Patho)physiological significance of the serum- and glucocorticoid-inducible kinase isoforms. *Physiol. Rev.* 86:1151–1178. https://doi.org/10.1152/physrev.00050.2005

Lew, D.J., and S. Kornbluth. 1996. Regulatory roles of cyclin dependent kinase phosphorylation in cell cycle control. *Curr. Opin. Cell Biol.* 8:795–804. https://doi.org/10.1016/S0955-0674(96)80080-9

Lien, E.C., C.C. Dibble, and A. Toker. 2017. PI3K signaling in cancer: beyond AKT. *Curr. Opin. Cell Biol.* 45:62–71. https://doi.org/10.1016/j.ceb.2017.02.007

Lindqvist, A., V. Rodríguez-Bravo, and R.H. Medema. 2009. The decision to enter mitosis: feedback and redundancy in the mitotic entry network. *J. Cell Biol.* 185:193–202. https://doi.org/10.1083/jcb.200812045

Liu, D., X. Yang, and Z. Songyang. 2000. Identification of CISK, a new member of the SGK kinase family that promotes IL-3-dependent survival. *Curr. Biol.* 10:1233–1236. https://doi.org/10.1016/S0960-9822(00)00733-8

Malik, N., T. Macartney, A. Hornberger, K.E. Anderson, H. Tovell, A.R. Prescott, and D.R. Alessi. 2018. Mechanism of activation of SGK3 by growth factors via the Class 1 and Class 3 PI3Ks. *Biochem. J.* 475:117–135. https://doi.org/10.1042/BCJ20170650

Maller, J.L., and E.G. Krebs. 1977. Progesterone-stimulated meiotic cell division in *Xenopus* oocytes. Induction by regulatory subunit and inhibition by catalytic subunit of adenosine 3′:5′-monophosphate-dependent protein kinase. *J. Biol. Chem.* 252:1712–1718.

Masui, Y. 1985. Meiotic arrest in animal oocytes. In: *Biology of Fertilization*. Academic Press, San Diego, CA; 189–219.

Maton, G., C. Thibier, A. Castro, T. Lorca, C. Prigent, and C. Jessus. 2003. Cdc2-cyclin B triggers H3 kinase activation of Aurora-A in *Xenopus* oocytes. *J. Biol. Chem.* 278:21439–21449. https://doi.org/10.1074/jbc.M300811200

Meijer, L., and P. Guerrier. 1984. Maturation and fertilization in starfish oocytes. *Int. Rev. Cytol.* 86:129–196. https://doi.org/10.1016/S0074-7696(08)60179-5

Minshull, J., A. Murray, A. Colman, and T. Hunt. 1991. *Xenopus* oocyte maturation does not require new cyclin synthesis. *J. Cell Biol.* 114:767–772. https://doi.org/10.1083/jcb.114.4.767

Nebreda, A.R., and I. Ferby. 2000. Regulation of the meiotic cell cycle in oocytes. *Curr. Opin. Cell Biol.* 12:666–675. https://doi.org/10.1016/S0955-0674(00)00150-2

Nurse, P. 1990. Universal control mechanism regulating onset of M-phase. *Nature.* 344:503–508. https://doi.org/10.1038/344503a0

O'Farrell, P.H. 2001. *Triggering the all-or-nothing switch into mitosis. Trends Cell Biol.* 11:512–519. https://doi.org/10.1016/S0962-8924(01)02142-0

Okano-Uchida, T., T. Sekiai, K. Lee, E. Okumura, K. Tachibana, and T. Kishimoto. 1998. *In vivo* regulation of cyclin A/Cdc2 and cyclin B/Cdc2 through meiotic and early cleavage cycles in starfish. *Dev. Biol.* 197: 39–53. https://doi.org/10.1006/dbio.1998.8881

Okano-Uchida, T., E. Okumura, M. Iwashita, H. Yoshida, K. Tachibana, and T. Kishimoto. 2003. Distinct regulators for Plk1 activation in starfish meiotic and early embryonic cycles. *EMBO J.* 22:5633–5642. https://doi.org/10.1093/emboj/cdg535

Okumura, E., T. Sekiai, S. Hisanaga, K. Tachibana, and T. Kishimoto. 1996. Initial triggering of M-phase in starfish oocytes: a possible novel component of maturation-promoting factor besides cdc2 kinase. *J. Cell Biol.* 132:125–135. https://doi.org/10.1083/jcb.132.1.125

Okumura, E., T. Fukuhara, H. Yoshida, S. Hanada, R. Kozutsumi, M. Mori, K. Tachibana, and T. Kishimoto. 2002. Akt inhibits Myt1 in the signalling pathway that leads to meiotic G2/M-phase transition. *Nat. Cell Biol.* 4: 111–116. https://doi.org/10.1038/ncb741

Ookata, K., S. Hisanaga, T. Okano, K. Tachibana, and T. Kishimoto. 1992. Relocation and distinct subcellular localization of p34cdc2-cyclin B complex at meiosis reinitiation in starfish oocytes. *EMBO J.* 11:1763–1772. https://doi.org/10.1002/j.1460-2075.1992.tb05228.x

Pahlavan, G., Z. Polanski, P. Kalab, R. Golsteyn, E.A. Nigg, and B. Maro. 2000. Characterization of polo-like kinase 1 during meiotic maturation of the mouse oocyte. *Dev. Biol.* 220:392–400. https://doi.org/10.1006/dbio.2000.9656

Pearce, L.R., D. Komander, and D.R. Alessi. 2010. The nuts and bolts of AGC protein kinases. *Nat. Rev. Mol. Cell Biol.* 11:9–22. https://doi.org/10.1038/nrm2822

Qian, J., C. Winkler, and M. Bollen. 2013. 4D-networking by mitotic phosphatases. *Curr. Opin. Cell Biol.* 25:697–703. https://doi.org/10.1016/j.ceb.2013.06.005

Rieder, C.L. 2011. Mitosis in vertebrates: the G2/M and M/A transitions and their associated checkpoints. *Chromosome Res.* 19:291–306. https://doi.org/10.1007/s10577-010-9178-z

Sadler, K.C., and J.V. Ruderman. 1998. Components of the signaling pathway linking the 1-methyladenine receptor to MPF activation and maturation in starfish oocytes. *Dev. Biol.* 197:25–38. https://doi.org/10.1006/dbio.1998.8869

Shilling, F., K. Chiba, M. Hoshi, T. Kishimoto, and L.A. Jaffe. 1989. Pertussis toxin inhibits 1-methyladenine-induced maturation in starfish oocytes. *Dev. Biol.* 133:605–608. https://doi.org/10.1016/0012-1606(89)90063-8

Tachibana, K., D. Tanaka, T. Isobe, and T. Kishimoto. 2000. c-Mos forces the mitotic cell cycle to undergo meiosis II to produce haploid gametes. *Proc. Natl. Acad. Sci. USA.* 97:14301–14306. https://doi.org/10.1073/pnas.97.26.14301

Terasaki, M., E. Okumura, B. Hinkle, and T. Kishimoto. 2003. Localization and dynamics of Cdc2-cyclin B during meiotic reinitiation in starfish oocytes. *Mol. Biol. Cell.* 14:4685–4694. https://doi.org/10.1091/mbc.e03-04-0249

Thomas, Y., L. Cirillo, C. Panbianco, L. Martino, N. Tavernier, F. Schwager, L. Van Hove, N. Joly, A. Santamaria, L. Pintard, and M. Gotta. 2016. Cdk1 Phosphorylates SPAT-1/Bora to promote Plk1 activation in *C. elegans* and human cells. *Cell Reports.* 15:510–518. https://doi.org/10.1016/j.celrep.2016.03.049

Towbin, H., T. Staehelin, and J. Gordon. 1979. Electrophoretic transfer of proteins from polyacrylamide gels to nitrocellulose sheets: procedure and some applications. *Proc. Natl. Acad. Sci. USA.* 76:4350–4354. https://doi.org/10.1073/pnas.76.9.4350

Tsao, P.I., and M. von Zastrow. 2001. Diversity and specificity in the regulated endocytic membrane trafficking of G-protein-coupled receptors. *Pharmacol. Ther.* 89:139–147. https://doi.org/10.1016/S0163-7258(00)00107-8

Vanhaesebroeck, B., J. Guillermet-Guibert, M. Graupera, and B. Bilanges. 2010. The emerging mechanisms of isoform-specific PI3K signalling. *Nat. Rev. Mol. Cell Biol.* 11:329–341. https://doi.org/10.1038/nrm2882

Vigneron, S., L. Sundermann, J.C. Labbé, L. Pintard, O. Radulescu, A. Castro, and T. Lorca. 2018. Cyclin A-cdk1-dependent phosphorylation of Bora is the triggering factor promoting mitotic entry. *Dev. Cell.* 45:637–650.e7. https://doi.org/10.1016/j.devcel.2018.05.005

Virbasius, J.V., X. Song, D.P. Pomerleau, Y. Zhan, G.W. Zhou, and M.P. Czech. 2001. Activation of the Akt-related cytokine-independent survival kinase requires interaction of its phox domain with endosomal phosphatidylinositol 3-phosphate. *Proc. Natl. Acad. Sci. USA.* 98:12908–12913. https://doi.org/10.1073/pnas.221352898

Webster, M.K., L. Goya, Y. Ge, A.C. Maiyar, and G.L. Firestone. 1993. Characterization of sgk, a novel member of the serine/threonine protein kinase gene family which is transcriptionally induced by glucocorticoids and serum. *Mol. Cell. Biol.* 13:2031–2040. https://doi.org/10.1128/MCB.13.4.2031